View metadata, citation and similar papers at core.ac.uk

brought to you by CORE

provided by Elsevier - Publisher Connector

Pergamon

Computers Math. Applic. Vol. 34, No. 2–4, pp. 229–244, 1997
Copyright©1997 Elsevier Science Ltd
Printed in Great Britain. All rights reserved
0898-1221/97 $17.00 + 0.00

PII: S0898-1221(97)00125-9

One Mechanism of Appearance of a Spiral Quasiattractor Involving Heteroclinic Contours

V. V. Bykov
Institute for Applied Mathematics & Cybernetics
Ul'janova st. 10, 603005, Nizhny Novgorod, Russia
bykov@focus.nnov.su

Abstract—Bifurcations and the structure of limit sets are studied for a three-dimensional van der Pol-Duffing system with a cubic nonlinearity. On a base of both computer simulations and theoretical results a model map is proposed which allows one to follow the evolution in the phase space from a simple (Morse-Smale) structure to chaos. It is established that appearance of complex, multistructural set of double-scroll type is stipulated by the presence of a heteroclinic orbit of intersection of the unstable manifold of a saddle periodic orbit and stable manifold of an equilibrium state of saddle-focus type.

Keywords—Bifurcation, Heteroclinic orbit, Chaos, Hyperbolic set.

1. INTRODUCTION

Nowadays, there exists a specific interest to the study of dynamical systems with chaotic behavior. The stimulating factor is that the phenomenon of dynamical chaos is typical in a sense and it is found in many applications. Usually, there appear difficulties with the answer to the following question: which limit sets the stochastic behavior is connected with and what is the mechanism of the transition from regular oscillations to the stochastic regime? Rigorously, the mathematical image of stochastic oscillations may be an attractive transitive limit set consisting of unstable orbits, that is a strange attractor. The well-known example is Lorenz attractor [1,2].

However, very often the appearance of chaos is connected with more complicated mathematical object: with a limit set containing nontrivial hyperbolic sets as well as stable periodic orbits (the latter may be invisible due to small absorbing domains and large periods). Such limit sets may generate stochastic oscillations because of the presence of perturbations stipulated by the inevitable presence of noise in experiments and by round-off errors in computer modelling. These limit sets are known as *quasiattractors* [3,4].

A typical example of a quasiattractor is the so-called Rossler attractor arising after a period-doubling cascade. Another example is the spiral attractor which, somehow, is a union of the Rossler attractor and the unstable limit set near a homoclinic loop of a saddle-focus [5]. Also, if two spiral quasiattractors unite including the saddle-focus together with its invariant unstable manifold, then a more complicated set arise which is called *double-scroll* [6].

The quasiattractors listed above are not abstract mathematical objects but they correspond to real processes visible in experiments as well as in computer simulations with, for instance, well-known Chua circuit (Figure 1). The study of this circuit was mainly carried out for the case of piecewise linear approximation of the nonlinear element [7–9]. Note that the interest

This research was supported in part by the EC-Russia Collaborative Project ESPRIT P 9282-ACTCS and by the ISF Grants R98000–R98300 and Russian Foundation of Basic Reseaches, Grant 97-01-00015.

Typeset by $\mathcal{A}\mathcal{M}\mathcal{S}$-TEX

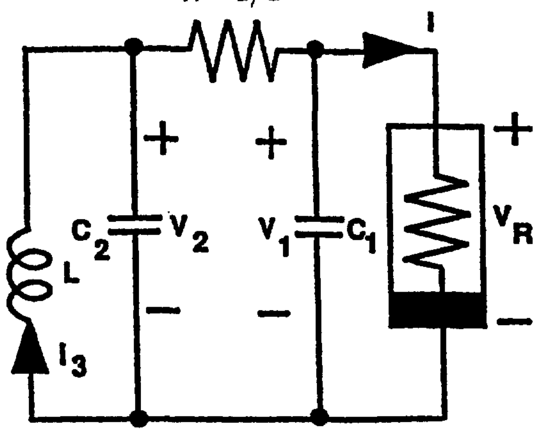

Figure 1. Circuit diagram for the chaotic van der Pol-Duffing oscillator.

to the piecewise linear representation is, apparently, connected not with the technical aspect of the problem but with the idea of the applicability of analytical methods for this case. It happened so, nevertheless, that the complexity of the analytical expressions arising here is too high, the immediate analysis of them is quite difficult and it cannot actually be done without use of numerical methods. In fact, the direct computer simulations of the differential equations has appeared to be more effective. Note also that the piecewise linear approximation does not allow one to use the full capacity of the methods and results of the bifurcation theory developed mostly for smooth dynamical systems. All this was the reason why the characteristic of the nonlinear element was modelled in [10] by a cubic polynomial which retains main geometrical features of the piecewise linear approximation. This choice gave the possibility to study local bifurcations by analytical methods, and then, by numerical simulation to show the presence of global bifurcations, in particular, those which indicate chaotic dynamic.

The scope of the present paper is to study main bifurcations and the structure of limit sets for the following three-dimensional system:

$$\dot{x} = \beta(g(y-x) - h(x)), \qquad \dot{y} = g(x-y) + z, \qquad \dot{z} = -y, \tag{1.1}$$

where β, g, α are positive parameters describing the aforementioned electronic circuit for the cubical $h(x) = \alpha x(x^2 - 1)$ approximation of the nonlinear element. The parameters β and g are connected with the physical parameters of the circuit: $\beta = C_1/C_2$, $g = G/\omega C_1$, where $\omega = 1/\sqrt{LC_2}$.

In spite of intensive theoretical and experimental studies, the question on principal bifurcations which the birth of the double-scroll quasiattractor in the model is connected with is not quite clear till now. The usual explanation based on Shil'nikov theorem [11] concerning with the bifurcation of saddle-focus homoclinic loops is not completely satisfactory here because the hyperbolic set lying near the loop is not attractive. Therefore, the establishing of the presence of such loops is not sufficient for the existence of chaotic attractor. It will be shown, for instance, that for system (1.1), there exists a region in the parameter space where the bifurcational set corresponding to a single-round homoclinic loop of a saddle-focus lie, and Shil'nikov conditions are satisfied, but there is no chaotic attractor and most of orbits tend to a stable limit cycle.

In the present paper, there is established that the appearance of the double-scroll is connected with the presence of heteroclinic orbits of intersection of two-dimensional invariant manifolds of the saddle-focus and a saddle periodic orbit. In one case, this is one of periodic orbits lying in the Rossler attractor; it also may be a symmetric periodic orbit arising through a condensation of orbits. This assertion is based on the study of a model map by the use of which the birth and the structure of an attractive limit set can be described which is the intersection of the double-scroll with a cross-section.

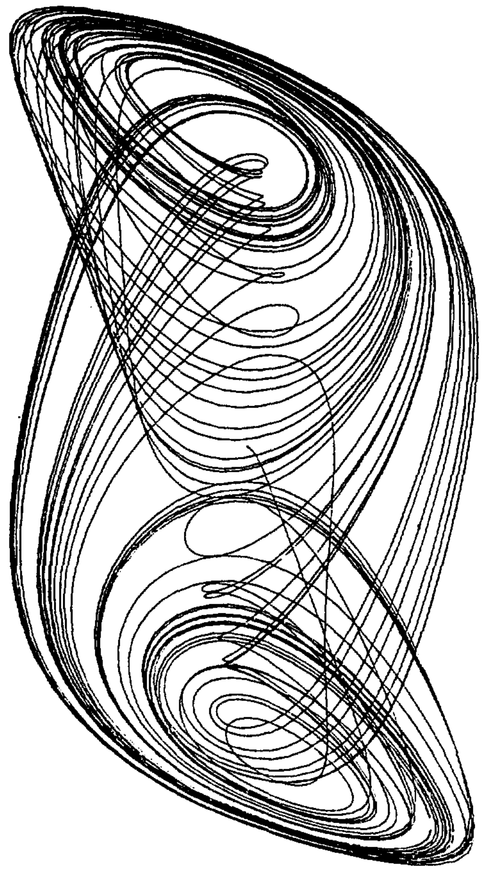

Figure 2. The double-scroll quasiattractor.

Note that the double scroll contains the saddle-focus which may have homoclinic loops; also, the double-scroll may contain structurally unstable homoclinic orbits of saddle periodic orbits. By virtue of [12–14], this implies that stable periodic orbits may appear in the double-scroll and it is, therefore, a quasiattractor [15]. This is the reason why the bifurcational set which corresponds to the birth of the double-scroll and which is a smooth curve contains a Cantor set of points of intersection with bifurcational curves corresponding to the situation where the one-dimensional separatrix of the saddle-focus belongs to the stable manifold of some nontrivial hyperbolic set. In the adjoint intervals, the separatrix, apparently, tends to one of the stable periodic orbits. A component of the bifurcational curve of the birth of the double-scroll can also be found which corresponds to the tangency of the stable and unstable manifolds of the hyperbolic set.

2. THE SCENARIO OF TRANSITION TO CHAOS

2.1. Local Bifurcations

Consider the sequence of the basic bifurcations with which the appearance of complex limit sets is connected. We begin with the study of equilibrium states. When $g > \alpha$, there exists only one equilibrium state O in the origin. When $g < \alpha$, there also exist two symmetric equilibrium states O_1, O_2 with the coordinates $x^*_{1,2} = \pm\sqrt{1 - g/a}$, $y^* = 0$, $z^*_{1,2} = \mp\sqrt{1 - g/\alpha}$. In this region of the parameter space, O is unstable: it is a saddle or a saddle-focus with one positive characteristic exponent. The one-dimensional separatrices of O will be denoted as P_i, $i = 1, 2$, and two-dimensional stable manifold of O will be denoted as $W^s(O)$.

On the line $g = \alpha$, the characteristic equation of 0 has one zero root for $\beta \neq 1/\alpha^2$ and it has two zero roots at $\beta = 1/\alpha^2$. We denote this point on the parameter plane $(\beta, g/\alpha)$ as TH

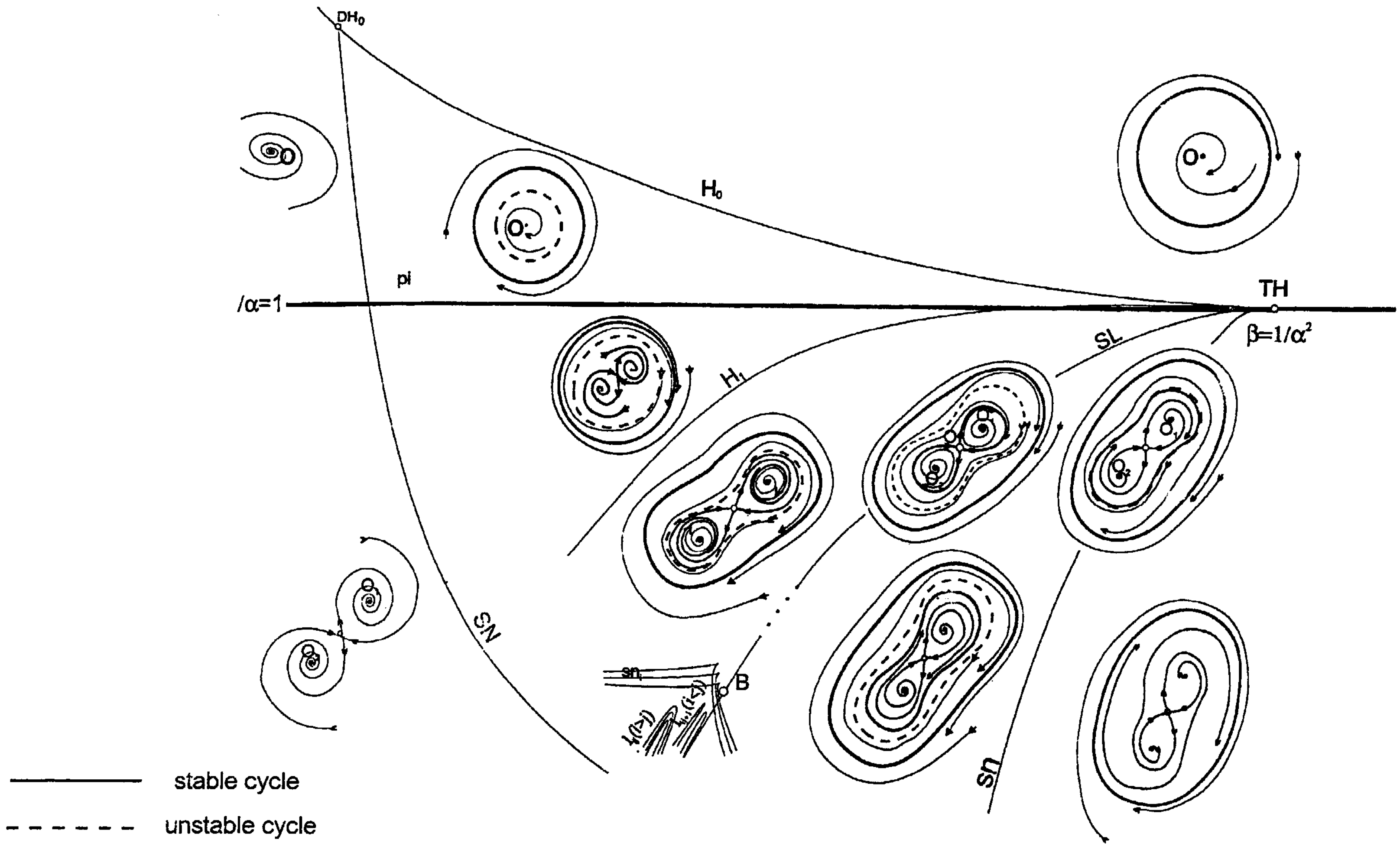

Figure 3. The local bifurcation diagram on the $\beta - g/a$ plane at $a = 0.2$. Three codimension-2 bifurcation points (TH, Takens-Harozov; DH_0, a degenerate Andronov-Hopf bifurcation of the origin; B, Bel'jakov point—a homoclinic loop to a saddle-focus with the saddle index ν equal to 1) and several codimension-1 bifurcation curves (PI, pitchfork of equilibria; H_0, Andronov-Hopf of the origin; H_1, Andronov-Hopf of nontrivial equilibria; SN and sn, saddle-node bifurcation of periodic orbits; SL-homoclinic loop of the origin) are present.

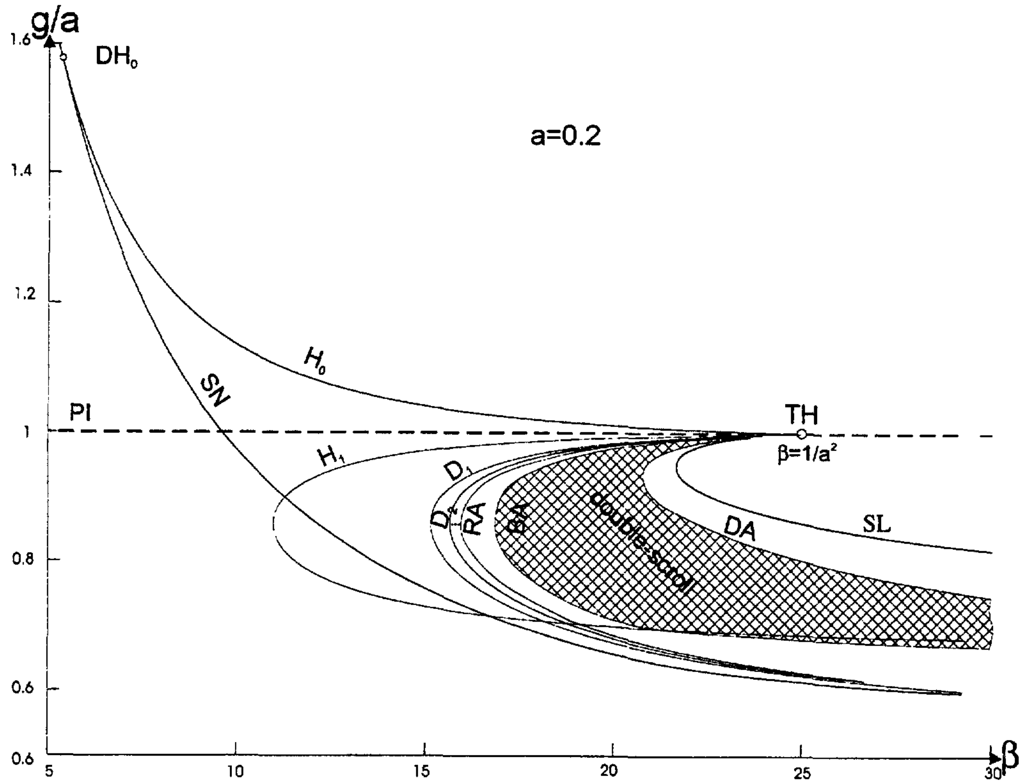

Figure 4. The global bifurcation diagram on $\beta - g/a$ plane at $a = 0.2$. The points TH, DH_0 and the curves H_0, H_1, SN, sn, and SL are the same as in Figure 3. The curve D_1 is the curve of a period-doubling, D_2 is the curve of secondary period-doubling, Ra is the curve of the birth of Rossler attractor as a result of an infinite sequence of period-doublings, Ba is the curve of the birth of the double-scroll quasiattractor, and Da is the curve of the death of the double-scroll.

(Takens-Harozov). The bifurcations in a neighborhood of this point are known [16,17] to be determined by the following normal form on the center manifold:

$$\dot{x} = y, \qquad \dot{y} = \epsilon x + \mu y + a x^3 + \gamma x^2 y.$$

In our case, for system (1.1), we have $a = -1/\alpha^2$, $\gamma = 3(\alpha^2 - 1)/\alpha^3$, and the bifurcation diagram corresponding to $\alpha < 1$ has the form shown in Figure 3 [16,17]. Note the presence of the curve SL which corresponds to a homoclinic loop of the saddle O. In a sufficiently small neighborhood of the point TH, the saddle value is negative in O, so a stable limit cycle is born from the loop. This cycle coalesces with an unstable cycle on the curve sn which corresponds to the saddle-node periodic orbit. All bifurcational curves starting with the point TH are continued outside its small neighborhood.

2.2. The Bifurcation Diagram

Let us now consider nonlocal bifurcations. A calculation of the first Lyapunov value $L(\beta)$ on the curve H_0 shows that there exists a point DH_0 where the Lyapunov value vanishes. On the segment TH-DH_0, we have $L(\beta) > 0$, and $L(\beta) < 0$ above the point DH_0. A bifurcation curve SN that corresponds to a symmetric periodic orbit with one multiplier equal to $+1$ goes from the point DH_0. To the right of this curve, there exist two symmetric periodic orbits: the stable periodic orbit Γ_0 and the saddle periodic orbit L_0. When moving on the parameter plane near the point TH, the latter disappears on the curve SL (in the region $g < \alpha$).

The bifurcation diagram is shown in Figure 4. The main phenomena mentioned above are connected with the curve SL. There exists a bifurcation point B on SL which correspond to the saddle exponent $\nu = -\operatorname{Re}\lambda_{1,2}/\lambda_3$ equal to unity where $\lambda, \lambda_{1,2}$ are the characteristic exponents of the saddle-focus 0. According to [18], below the point B there exists a nontrivial hyperbolic set in a neighborhood of the homoclinic loop of the saddle-focus. It follows from [18] that below the point B, there exist infinitely many bifurcational curves l_{ij} and l_{ij+1} corresponding to multiround homoclinic loops and infinitely many bifurcational curves sn_i corresponding to saddle-node periodic orbits.

Different types of bifurcation sequences leading to chaotic dynamics were described in [5]. In our case, one of the typical scenarios can be: equilibrium state—periodic orbit—period doubling—chaos, as well as the scenario connected with structurally unstable Poincaré homoclinic orbits arising before the period-doubling cascade finishes (see, for instance, [19]).

We describe here (following [5]) the main features of the first scenario. We will trace the periodic orbit P_i which is born from O_i. Note that P_i is the boundary of the unstable manifold $W^u(O_i)$; it is also the limit set for a separatrix of the saddle-focus O. Later (when the parameter β increases) the multipliers of this periodic orbit become complex-conjugate which leads to that the manifold $W^u(O_i)$ become winding onto P_i. Next, on the curve D_1, the period-doubling bifurcation happens with the orbit Γ_i, and then the period-doubling cascade starts. This process leads to the appearance of two nonsymmetric Rossler attractors $\mathcal{M}_1$ and $\mathcal{M}_2$ which inherit to P_1 and P_2.

In the parameter region where the quasiattractor $\mathcal{M}_i$ is separated from the other by the stable manifold $W^s(0)$, it is a limit set for $W^u(O_i)$ as well as for the one-dimensional separatrix Γ_i. The beginning of the birth of a symmetric quasiattractor is the tangency of $W^u(O_1)$ with $W^s(O)$ along a heteroclinic orbit (due to the symmetry, there appears also a heteroclinic orbit of tangency of $W^u(O_2)$ with $W^s(O)$). When the parameter varies, each of this heteroclinic orbits splits onto two transverse heteroclinic curves. In this situation, both one-dimensional separatrices Γ_1 and Γ_2 of the saddle-focus O belong simultaneously to the boundary of each of the manifolds $W^u(O_i)$.

3. THE MODEL MAP

In this section, we propose a geometric model which reflects main features of system (1.1). On the other hand, our construction is interesting itself and it may be considered as a realization of the object called "confinor" in [20,21].

Suppose that smooth dissipative system X possessing a center symmetry has a saddle-focus equilibrium state O with the characteristic exponents $\lambda_{1,2} = -\lambda \pm i\omega$, λ_3, where λ, ω, and λ_3 are positive. Also, the system is supposed to have a symmetric saddle periodic orbit L_0. Assume that the stable manifold $W^s(L_0)$ of the periodic orbit is homeomorphic to a cylinder and the saddle-focus O lies inside the cylinder. We also suppose that outside $W^s(L_0)$ there is a stable symmetric periodic orbit Γ_0, as in system (1.1).

Let D be some cross-section on which Cartesian coordinates (x, y) can be introduced such that the line $l_0 : y = 0$ is the intersection with the manifold $W^s(O)$. Denote as p_i the point of first intersection of the one-dimensional separatrix Γ_i of O with D. Let $U(l_0)$ and $U_i(p_i)$ be some neighborhoods of the line l_0 and of the point p_1, respectively, and let $U^+(l_0)$ ($U^-(l_0)$) be the component of $U(l_0)$ corresponding to the positive (respectively, negative) values of y. According to [13,15], the map $U^+(l_0) \to U_1(p_1)$ defined by the orbits of the system is represented in the form

$$\begin{aligned} \bar{x} &= x^* + b_1 \cdot x \cdot y^\nu \cos(\omega \cdot \ln(y) + \theta_1) + \psi_1(x, y), \\ \bar{y} &= y^* + b_2 \cdot x \cdot y^\nu \sin(\omega \cdot \ln(y) + \theta_2) + \psi_2(x, y), \end{aligned} \tag{3.1}$$

where ψ_i are smooth functions which tend, as $y \to 0$, to zero along with their first derivative with respect to y. An analogous formula is valid for the map $U^-(l_0) \to U_2(p_2)$. An extrapolation of the properties of the local map defined by (3.1) leads to the following construction which is in a good agreement with the results of computer simulations.

Consider two components D^+ and D^- into which the cross-section D is divided by the line l_0; i.e., $D = D^+ \cup D^- \cup l_0$. We have $D^+ = \{(x,y) \mid |x| \le c,\ 0 < y \le h^*(x)\}$, $D^- = \{(x,y) \mid |x| \le c, -h(x) \le y < 0\}$, where $y = h^*(x)$ is a component of the intersection of the stable manifold $W^s(L_0)$ with D. The orbits of the system define the maps $T(\mu)^+ : D^+ \to D, T(\mu)^- : D^- \to D$, and $T(\mu)^+$ and $T(\mu)^-$ are written as

$$\bar{x} = f^+(x,y,\mu), \qquad \bar{y} = g^+(x,y,\mu)$$

and

$$\bar{x} = f^-(x,y,\mu), \qquad \bar{y} = g^-(x,y,\mu),$$

respectively; here, f^+, f^-, g^+, $g^- \in C^r$, and $\mu = (\mu^{(1)}, \mu^{(2)})$.

The following properties are assumed for these maps.

1. T^+ and T^- can be defined on l_0 so that $\lim_{y\to+0} T^+M(x,y) = (x^*,y^*)$, $\lim_{y\to-0} T^-M(x,y) = (x^{**}, -y^*)$, where $p_1(x^*,y^*)$ and $p_2(x^{**},-y^*)$ are the points of first intersection of the one-dimensional separatrices of the saddle-focus O with D. We suppose that T depends on μ in the following way: the first component of μ moves the point P_1 in vertical direction and the second component of μ moves it in horizontal direction.
2. Each of the areas D^+, D^- is represented as a union of an infinite number of regions $\tilde{S}_0^+$, $\tilde{S}_0^-$, S_i^+, S_i^-, $S_i^+ = \{(x,y) \mid |x| \le c,\ \xi_{i+1}^* \le y < \xi_i^*\}$, $S_i^- = \{(x,y) \mid |x| \le c, -\xi_i^* < y \le -\xi_{i+1}^*\}$, $i = 1,\dots,$ where $\xi_0^* = h^*(x)$, $\lim_{i\to\infty} |\xi_i^*| = 0$. The map T^+ or T^- acts so that the image of any vertical segment with one end-point on l_0 has the form of a spiral winding at the point p_1 or p_2, respectively. The boundary $\gamma_i^\pm : y = \xi_{i+1}^*$ of two adjoining regions $S_{i,}^\pm S_{i+1}^\pm$ is chosen such that $\frac{\partial \bar{y}}{\partial y} = 0$ if and only if $(x,y) \in \gamma_i^\pm$, and $T^\pm\gamma^\pm$ is a segment of a curve of the form $x = h_i(y)$ where $|\frac{dh}{dy}| =< 1$.

Introduce the following notations:

$$D_1 = \left\{(x,y) \mid -c \le x \le -\frac{c}{2}, |y| < h(x)\right\}, \quad D_2 = \left\{(x,y) \mid \frac{c}{2} \le x \le c, |y| < h(x)\right\},$$
$$D_i^+ = D^+ \bigcap D_i, \quad D_i^- = D^- \bigcap D_I,$$
$$T \equiv T^\pm \mid D^\pm, \quad (f^\pm, g^\pm) \equiv (f,g), \quad S_i \equiv S_i^\pm, \quad \gamma_i \equiv \gamma_i^\pm.$$

Let S_0^+ (S_0^-) be that part of $\tilde{S}_0^+$ $(\tilde{S}_0^-)$ on which $TS_0^+ \in D_1$ $(TS_0^- \in D_2)$. Suppose that the map T satisfies the following additional conditions:

3. $TD_1 \subset D, TD_2 \subset D$;
4. $|\frac{\partial \bar{x}}{\partial x}| < 1$;
5. $r_i = \varrho(T\gamma_i, T\gamma_{i+1}) > q\xi_i^*$, $q > 2$, $i > 1$;
6. in S_i there can be selected a set σ_i such that the following inequality is fulfilled everywhere on σ_i:
$$\|g_y\| > 1, \qquad 1 - \|f_x \cdot g_y^{-1}\| < 2\sqrt{\|f_y \cdot g_y^{-1}\| \cdot \|g_x \cdot g_y^{-1}\|};$$
7. $p_1 \in S_0^+$, $p_2 \in S_0^-$.

Note that Condition 2 is fulfilled near the line l_0 (i.e., for the sets S_i with i sufficiently large) by virtue of (3.1). Conditions 3–5 are also automatically fulfilled near l_0 if the saddle index $\rho = -\operatorname{Re}\lambda_{1,2}/\lambda_3$ is less than unity in the saddle-focus. Moreover, in this case $r_{i}/\xi_i^* \to \infty$ as $i \to \infty$; in other words, $q \to \infty$ as $i \to \infty$.[1]

The fulfillment of Condition 6 means that, for those parameter values for which there exist i and j such that the map $\sigma_i \to \sigma_j$ is defined, the operator $\mathcal{T}_{ij} : H_i(L) \to H_j(L)$ is contract-

[1]The validity of such a model can be verified by computer simulations. It occurs that the contraction in horizontal-direction is so strong that the images of the area $x = \sqrt{1 - g/a}/2$ under the action of the Poincaré map have, in natural scale, the form of one-dimensional curves (Figures 5b–8b,12b).

ing [22,23], where $H_i(L)$ is the space of the curves $y = \varphi(x)$ lying in σ_i and satisfying the Lipschitz condition with some Lipschitz constant L.

For system (1.1), one can see that the divergence $\mathrm{Div} = \beta(\alpha - g) - g$ of the vector field in the saddle-focus O is positive for $g < \beta\alpha/(1+\beta)$. This implies that $2\nu < 1$ in this parameter region. For us, it is important that $\nu < 1$ which, for the case of formation of a homoclinic loop, implies [11] the presence of nontrivial hyperbolic sets and infinitely many Smale horseshoes.

Let T_k be the restriction of T onto S_k. For those parameter values for which $T\gamma_0 \subset S_0, T\gamma_0 \cap S_1 = \emptyset$ (i.e., $T_0 S_0 \subset S_0$ as in Figure 5), in S_0 there exists a stable limit set which depends on the concrete properties of the map T_0. When parameter change so that the image of the boundary γ_0 moves down, with the moment when $T\gamma_0 \cap S_1 \neq \emptyset$, there appears the situation analogous to the creation of Smale horseshoe (Figure 6). In addition to the fixed point $M_1 = T_1 M_1$, saddle periodic points $M_{1k} = T_0^k \circ T_1 M_{1k}$, $1 < k \geq k^+$ arise in S_1 and S_0. The appearance of these points implies the creation of a nontrivial hyperbolic set due to formation of a heteroclinic contour composed by heteroclinic orbits of intersection of the stable (unstable) manifolds of each of these points with the unstable (stable) manifolds of each other point.

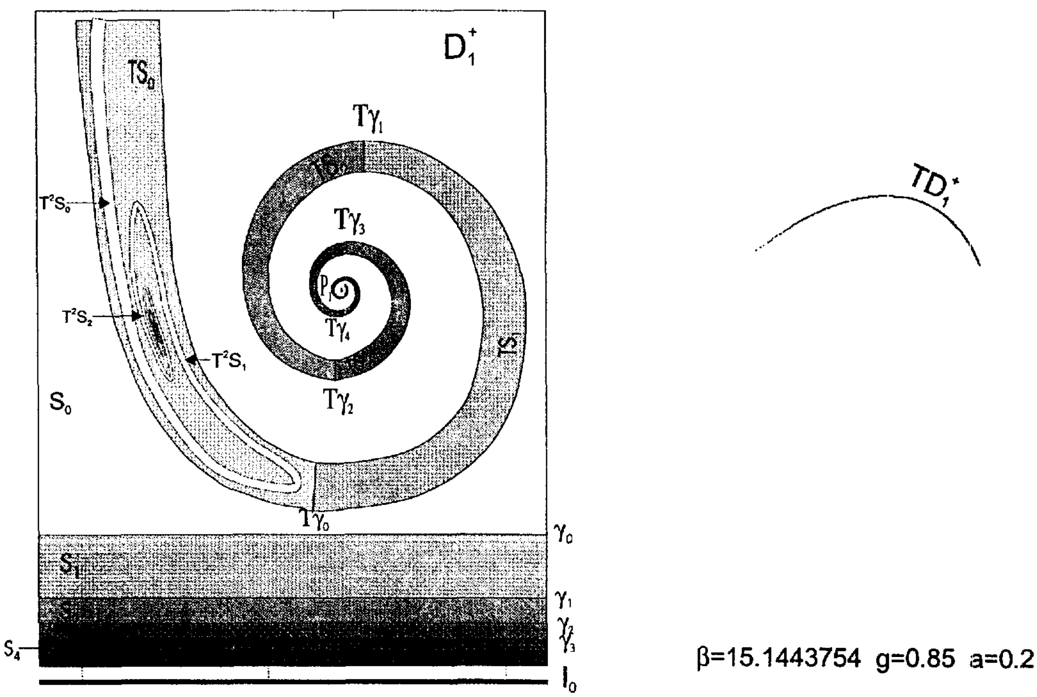

(a) The theoretical model. (b) Computer simulations.

Figure 5. The Poincaré map on the semiplane $x = \sqrt{(1-g/a)}$, $y > \sqrt{(1-g/a)}(\beta - 1/4)/2\beta$ for the parameter values lying to the left of the bifurcation curve D_1.

The further lowering of the curve $T\gamma_0$ implies the appearance of periodic points $M_{2n} = T_0^n \circ T_2 M_{2n}$ $n > k_2^-$ in S_0 and S_2, and so on. The structure of the limit set becomes more and more complicated but it remains in the region D_1^+ for the moment when the unstable manifold of the point M_{2n} will have a tangency with l_0 (Figure 7). After the moment of tangency of $T_0 S_0 \cap l_0 \neq \emptyset$ and $T_1 S_1 \cap l_0 \neq \emptyset$, there appear preimages $T_0^{-1} l_0$ and $T_1^{-1} l_0$ of the line l_0 in S_0 and S_1 near the boundary γ_0. These preimages intersect the unstable manifold of the nontrivial hyperbolic set. Thus, the preimages of l_0 will accumulate on the leaves of the stable manifold of the hyperbolic set. Besides, those parts of S_0^+ and S_1^+ which are bounded by the curves $T_0^{-1} l_0$ and $T_1^{-1} l_0$ are mapped by T^+ into D^- (i.e., in the region where the map T^- acts). Due to the symmetry, the analogous parts of S_0^- and S_1^- are mapped into D^+ by T^-. Thus, two symmetric attractors are

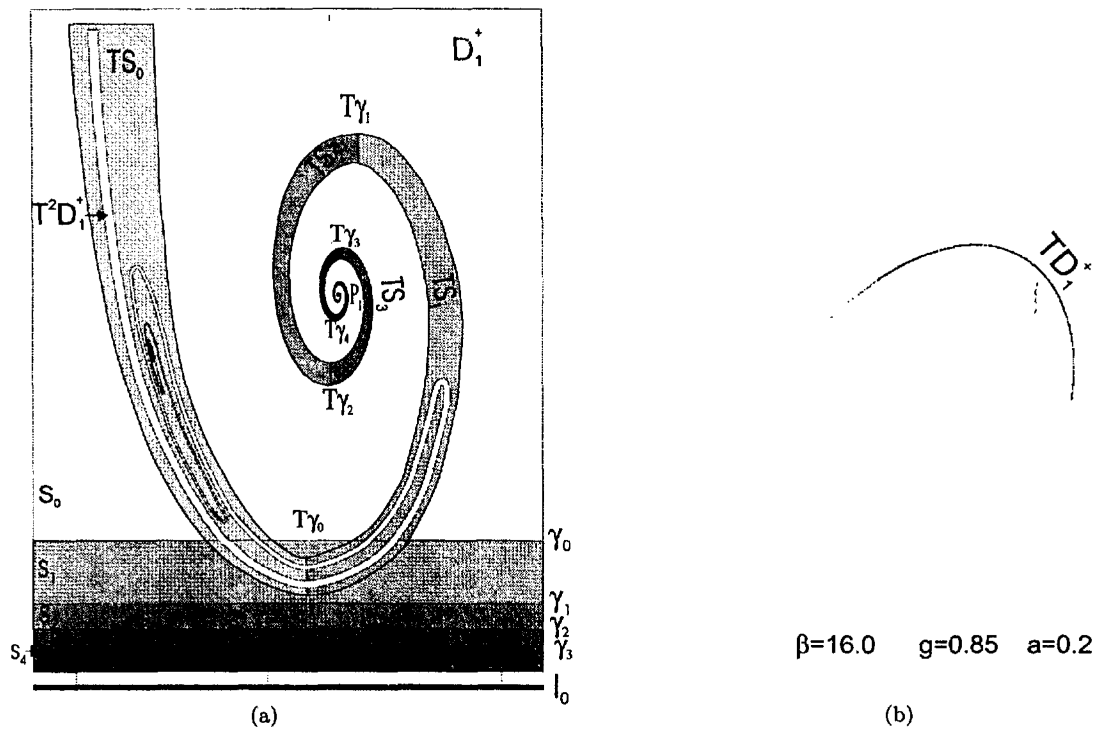

Figure 6. As Figure 5 with values of β and g/a lying to the right of the curve D_1.

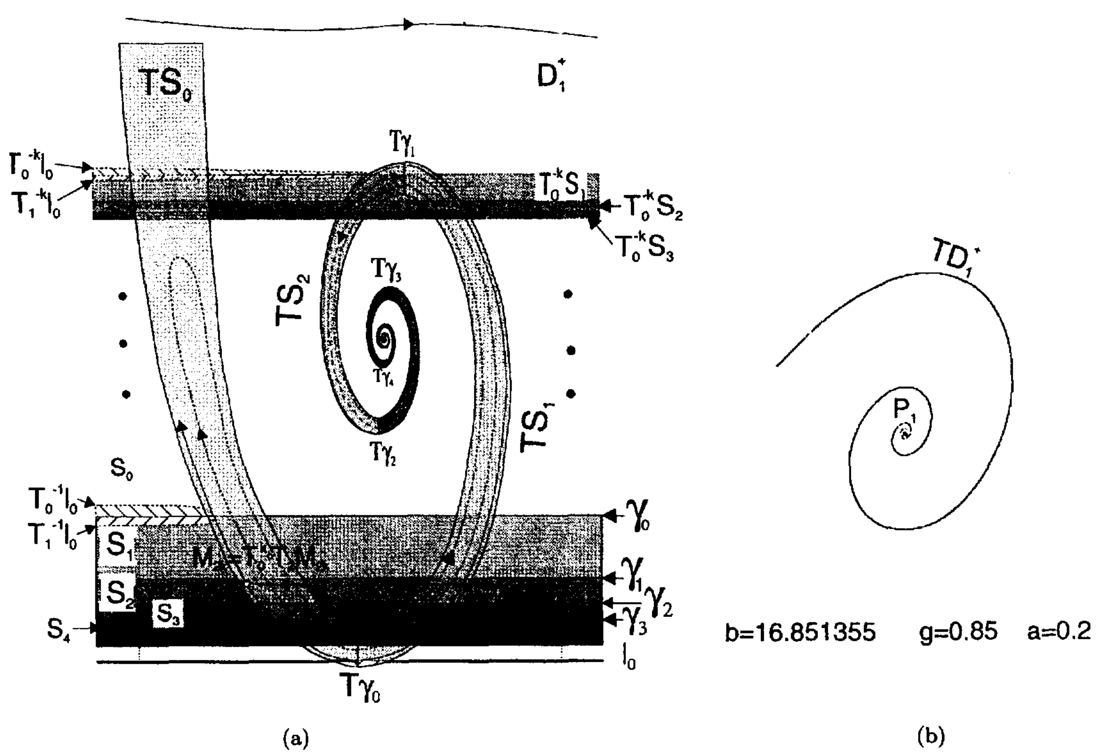

Figure 7. As Figure 5 with values of β and g/a lying on the curve BA.

now united (Figure 8). The limit set newly created is the double-scroll attractor which we will consider in the next section.

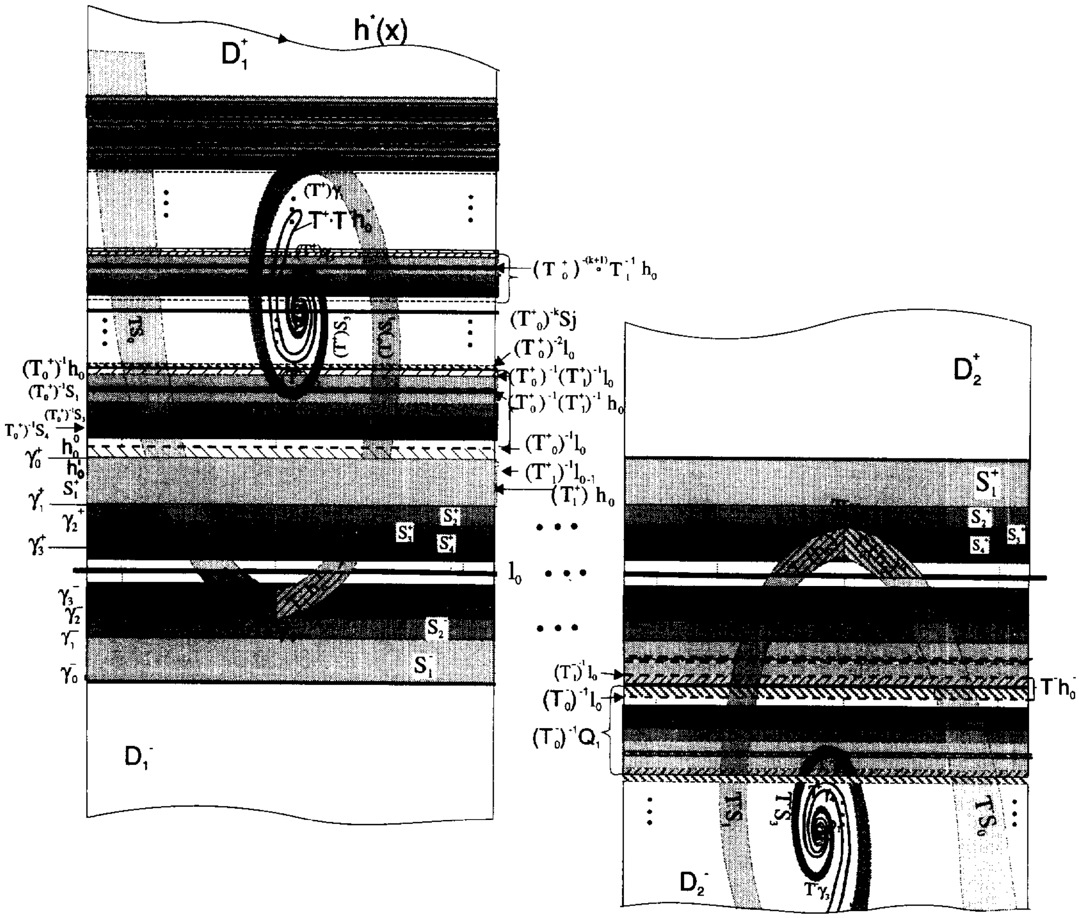

(a)

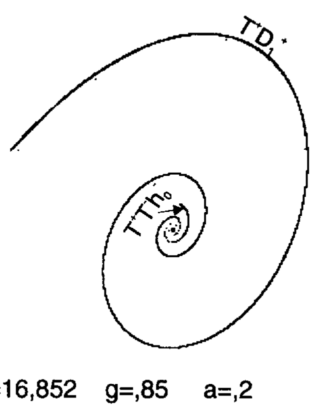

(b)

Figure 8. As Figure 5 with values $\beta, g/a$ lying to the right of the curve BA.

4. THE STRUCTURE OF THE LIMIT SET

Denote the region bounded by the lines $T_0^{-1}l_0$ and $T_1^{-1}l_0$ as h_0. Consider the regions

(a) h_0^0 and h_0^1 which are the connected components of $h_0\backslash\gamma_0$;

(b) $Q_1 = \cup_{i=1}^{\infty} S_i$.

Let $\bar{k}$ be the number such that the point p_1 belongs to $T_0^{-\bar{k}}(Q_1 \cup h_0^0)$. Denote

$$k_1^+ = \max\left\{k \mid T_0^{-k}\left(Q_1 \bigcup h_0^0\right) \cap T_1 S_1 \neq \emptyset,\ T\gamma_1 \cap T_0^{-k}\left(Q_1 \cup h_0^0\right) = \emptyset\right\}.$$

and

$$R_1 = S_1 \backslash \left(h_0^1 \bigcup_{k=1}^{k_1^+} \left(T_1^{-1} \circ T_0^{-k} \left(Q_1 \bigcup h_0^0 \right) \right) \right).$$

By these definitions, $k_1^+ > \bar{k}$ is the maximal number such that $T_1\gamma_1 \cap T_0^{-k_1^+}(Q_1 \cup h_0) = \emptyset$ and $T_1\gamma_1 \cap T_0^{-k_1^+-1}(Q_1 \cup h_0) \neq \emptyset$; and R_1 is the complement to the preimage of the regions $T_0^{-k}(Q1 \cup h_0^0)$ with respect to the map T_1.

Let $X \subset D_1^+$ be a region bounded by two vertical segments lying on the boundaries of D_1^+ and by two horizontal lines lying between $T\gamma_0$ and $T\gamma_1$. Let X_0 and X_1 be the intersections $TS_0 \cap X$ and $TS_1 \cap X$, respectively. If $T\gamma_i \cap X_j = \emptyset$, $i, j = 0, 1$, then the left and right boundaries of these sets again will lie on the corresponding boundaries of D_1^+.

We define inductively the subsets of D_1 such that if a point belongs to such subset, this will determine its behavior under the action of the map T.

(1) $X_i^0 = X_i$, $i = 0, 1$,
(2) $X_i^l = T_i^{-1}(X_i^{l-1} \cap TS_i)$.

Evidently, $X_i^{l_1}$ is the $l_1{}^{\text{th}}$ preimage of X_i with respect to T_i. Analogously to (1), we denote $X_i^{l_1} \cap TS_j = (X_i^{l_1})_j^1$. Applying $l_2 - 1$ times, the map T_j^{-1} we obtain, analogously to (2), the set $(X_i^{l_1})_j^{l_2}$, or omitting parentheses, $X_{i,j}^{l_1,l_2}$. Thus,

(3) $X_{n_1,n_l,\ldots,n_{l-1},n_l}^{m_1,m_2,\ldots,m_{l-1},1} = T_{n_l}^{-1}(X_{n_1,n_2,\ldots,n_{l_1-1}}^{m_1,m_2,\ldots,m_{l-1}} \cap TS_{n_l})$, where $n_i = 0, 1$; $0 \leq m_i \leq k_1^+$ if $n_i = 0$, and $m_i \in \mathbf{z}$ if $n_i = 1$.

The set of regions defined by (3) is in one-to-one correspondence with the set of infinite (to the left) sequences of zeros and units with the restriction that the length of complete strings of zeros must not be greater than k_1^+ (because $m_j \leq k_1^+$ if $n_j = 0$; see (3)).

As the region X, one can, for instance, take the region S_1 because $S_1 \cap TS_0 \neq \emptyset$ and $S_1 \cap T_1S_1 \neq \emptyset$ in the situation, where $T\gamma_0$ lies below l_0. By the above scheme (1)–(3), the set $\{(S_1)_{\mathbf{m_s}}^{\mathbf{n_s}}\}$ of regions $(S_1)_{\mathbf{m_s}}^{\mathbf{n_s}}$ is constructed, where $\mathbf{m_s} = (m_1, m_2, \ldots, m_{i_s})$, $\mathbf{n_s} = (n_1, n_2, \ldots, n_s)$ are multi-indices. The limit $s \to \infty$ corresponds to a set S_1^* which is in one-to-one correspondence with the set of sequences infinite to the left, composed by zeros and units with the restriction that the length of any complete string of zeros does not exceed k_1^+.

The set S_1^* consists of invariant fibers; it can also be shown by the use of Condition 6 that the set S_1^* contains a nontrivial hyperbolic set: each fiber contains exactly one point of this set. Note that the nonwandering set is not, in principle, exhausted by the orbits of S_1^*.

The following lemma describing the structure of the decomposition of S_1 onto regions corresponding to different types of orbit behavior is evident.

LEMMA 3.1. *The region S_1 is a union of the following sets:*

(a) S_1^**—the set of stable fibers; the set of points whose orbits never leave $S_0 \cup S_1$ under the action of the map T;*
(b) $H^* = h_0^1 \cup (\cup_{s\geq 1}^{\infty}(h_0)_{\mathbf{n}_s}^{\mathbf{m}_s} \cap S_1$*—the set of points whose orbits leave D_1^+ and enter D_1^- after a finite number of iterations;*
(c) $R_1^* = \cup(R_1)_{\mathbf{n}_s}^{\mathbf{m}_s}) \cap S_1$*—the set of points whose orbits enter R_1 after a finite number of iterations; this set may contain stable periodic orbits;*
(d) $Q_1^* = \cup_{s\geq 1}^{\infty}(Q_1 \backslash S_1)_{\mathbf{n}_s}^{\mathbf{m}_s} \cap S_1$*—the set of points whose orbits enter one of the regions S_i, $1 < i < \infty$ after a finite number of iterations; and*
(e) $L_1^* = \cup_{s\geq 1}^{\infty}(l_0)_{\mathbf{n}_s}^{\mathbf{m}_s} \cap S_1$*—the set of preimages of the discontinuity line l_0, where $\mathbf{m}_s = (m_1, m_2, \ldots, m_{j_s})$, $\mathbf{n}_s = (n_1, n_2, \ldots, n_s)$, $m_i \in \{0, 1\}$, $m_{j_s} = 1$; $1 \leq n_i \leq k_1^+$ if $m_i = 0$ un$_i \in \mathbf{Z}$, if $m_i = 1$.*

As it follows from Lemma 1, the sets $Q_1^* \cup H_1^* \cup R_1^*$ give the adjoint intervals in S_1 for the Cantor discontinuum of the set S_1^* of stable fibers of the nontrivial hyperbolic set. Evidently, if

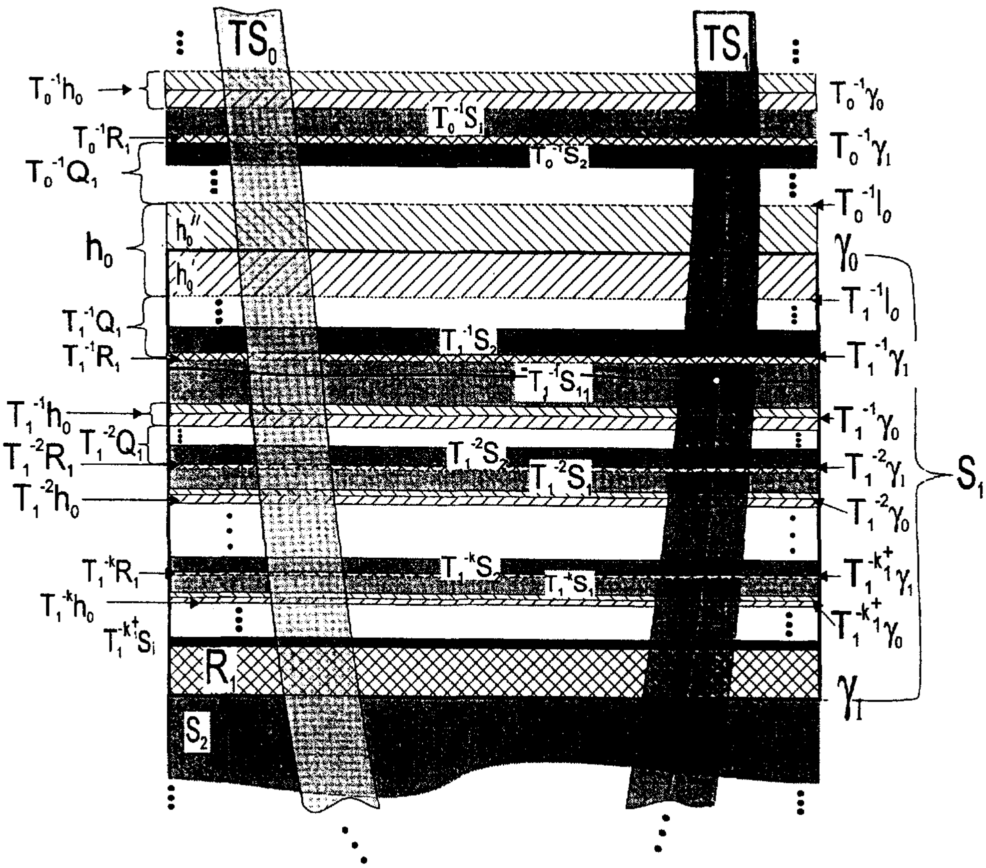

Figure 9. The decomposition of the region S_1 onto the regions corresponding to different behavior of orbits (an illustration to Lemma 3.1).

$p_1 \in H_1^*$, then after some number of iterations the point p_1 will lie below the line l_0 and the next part of its orbit will be defined by the map T^-. If $p_1 \in S_1^*$ (i.e., if it belongs to some stable fiber), then there exist arbitrarily small perturbations which move the point p_1 into H_1^*. Hereat, the point p_1 will cross preimages of the discontinuity line l_0. Thus, after a number of iterations, the point p_1 may be mapped close to the line l_0, at a distance which is less than perturbations present in the system, and the behavior of the following iterations of p_1 will not be defined uniquely.

For the set S_2, there can also be found the number k such that $T_0^{-k}(S_1 \cup S_2) \cap T_2 S_2 \neq \emptyset$ and $T_0^{-k}(S_1 \cup S_2) \cap T(\gamma_1 \cup \gamma_2) = \emptyset$. In this case, S_2 will contain the preimage $T_2^{-1} \circ T_0^{-k} S_1$, together with the preimages of the regions S_i, $i = 1, 2, \dots, h_0$ and $(R_1)_1^*$ defined by Lemma 1.

The same may hold for the other regions S_i; i.e., there exist $\bar{m}, j_i^*$ and k_i^-, k_i^+ $(1 \leq k_i^- \leq k_i^+$, $1 < i \leq \bar{m}$, $1 \leq j_i^* \leq i-1)$ such that the following situation takes place for $k_i^- \leq k \leq k_i^+$ and $1 < i \leq \bar{m}$: $T_0^{-k} S_j \cap T_i S_i \neq \emptyset$, $T_0^{-k}(\cup_{j_i^* \leq i} S_j) \cap T(\gamma_i \cup \gamma_{i+1}) = \emptyset$. As in Lemma 1, the decomposition of the region S_i onto the sets $S_i, h_0, S_i/\sigma_i$, $i = 1, 2, \dots, \bar{m}$, and $Q_m = \cup_{i=m}^{\infty} Q_i$ can be done. Note that any region S_i, $1 \leq i \leq \bar{m}$ will contain preimages of the regions S_j, $j \leq i$ (Figures 7–9).

To describe the set of preimages of the discontinuity line l_0 and the regions S_i, we consider the graph G defined in the following way [23]. Each region S_i is represented by the vertex a_i; the saddle-focus O is represented by the vertex 0 with the edge $\hat{O}$ which starts and ends in 0; the maps $T_j^{-1} \circ T_0^{-k} S_i$: $S_i \to S_j$ are represented by the edges $\hat{b}_{ij}^k$ if these maps are defined and if $T(\gamma_j \cup \gamma_{j+1}) \cap T_0^{-k} S_i = \emptyset$; if $T_0^{-k} l_0 \cap S_1 \neq \emptyset$ and $T_0^{-k} l_0 \cap T(\gamma_i \cup \gamma_{i+1}) = \emptyset$, then also the edges $\hat{1}$ and $\hat{2}$ are constructed (Figure 10).

Simultaneously, we consider the graph G_σ which obtained if to retain only that edges $\hat{b}_{ij}^k$ of G for which $T_j^{-1} \circ T_0^{-k} S_i \subset \sigma_j$. We also retain only those vertices for which there exist at least one

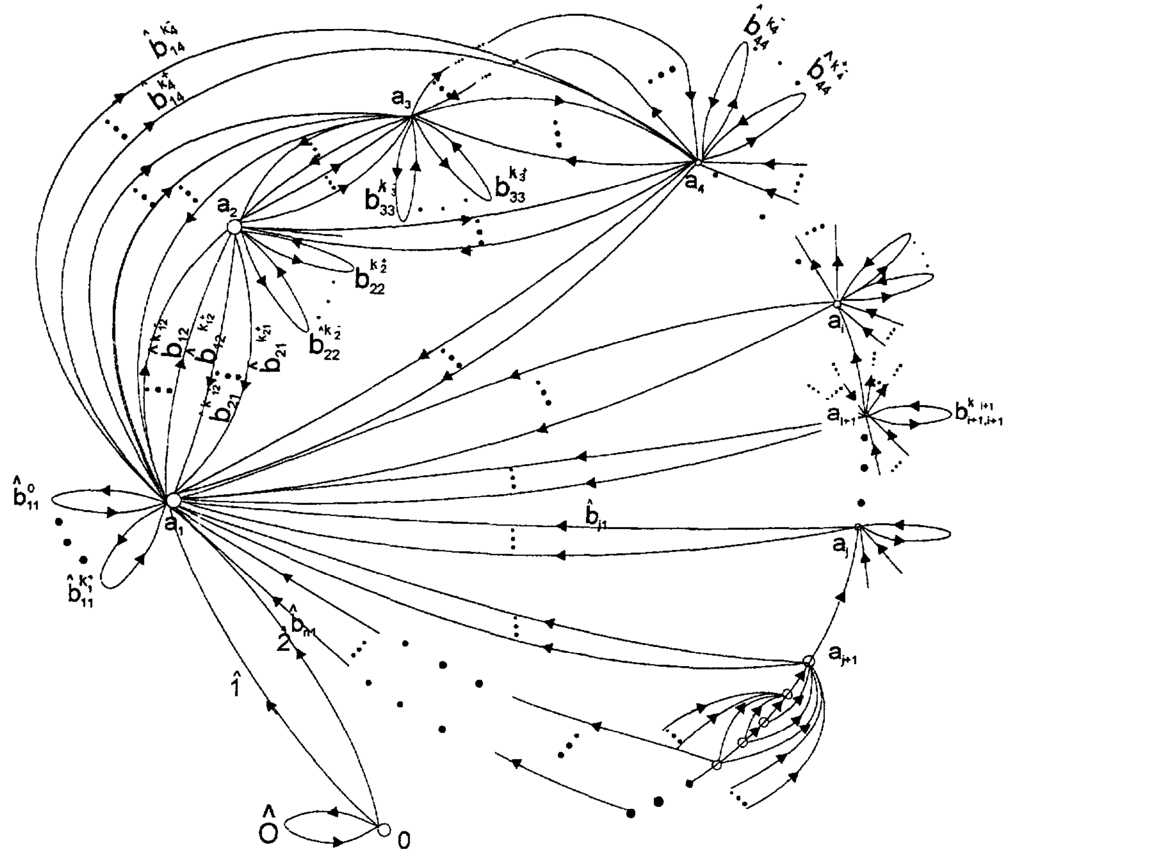

Figure 10. The graph G_σ.

edge entering the vertex and at least one edge leaving the vertex; all the other are eliminated with the adjoining edges.

By definition, each of the edges $\hat{b}^k_{ij}$ of G_σ corresponds to the map $T_j^{-1} \circ T_0^{-k} : \sigma_i \to \sigma_j$ which is saddle on σ_i by virtue of Condition 6. Due to [1,23], we arrive at the following theorem.

THEOREM 3.1. *The system X_μ has a nontrivial hyperbolic set which is in one-to-one correspondence with the set of infinite paths along the edges of G_σ.*

The next theorem shows the nontrivial character of the bifurcational set on the parameter μ plane.

THEOREM 3.2. *There exists a countable set of bifurcational curves corresponding to the presence of homoclinic loops of the saddle-focus O and a Cantor set of bifurcational curves corresponding to the situation where the one-dimensional separatrix of the saddle-focus lies on the stable manifold of a nontrivial hyperbolic set.*[2]

Proof. Let μ_0 be the value of μ at which $W^u(M_{2k})$ have a tangency with $W^s(0)$. Let μ vary so that the point $p_1(\mu)$ traces a vertical line v: $\mu^{(2)} = 0$, $\mu_0 < \mu < \mu^*$ such that on the upper bound of the line the point $p_1(\mu)$ belongs to the preimage of the upper bound of S_i, and on the lower bound of the line, the point P_1 belongs to the preimage $T_0^{-\bar{k}}\gamma_i$ of the lower bound of S_i. For all $\mu \in v$, we have $p_1(\mu) \in T_0^{-\bar{k}} S_i$, $i > 1$. By virtue of Condition 5, $T_0^{-k} S_j \cap T_i S_i \neq \emptyset$, $j \geq i$. Denote $T_i^{-1} \circ T_0^{-k}$ as T_{ik}. If $p_1(\mu) \in T_0^{-k} S_i$, this map is defined on the set $\cup_{j=i}^{\infty} S_j$, and the fixed point $M_{i\bar{k}} = T_i^{-1} \circ T_0^{-\bar{k}} M_{i\bar{k}}$ exists in S_i. We denote the stable manifold of this point as $W^s(M_i\bar{k})$. This stable invariant fiber is a topological limit for the preimages $T^n_{ik} S_j$, $J \geq i$. Evidently, the size of

[2]On the structure of the bifurcational set corresponding to homoclinic loops of systems close to a system with a saddle-focus homoclinic loop, see also [24].

the set $T^n_{ik}S_j$, $j \geq i$ tends to zero as $n \to \infty$. The preimages $T_{ik}S_j$, $j > i$ lie either below W^s_i, if the map $T^k_0 \circ T_i$ acts in an orientable way (i is even), or from both sides if the map $T^k_0 \circ T_i$ is nonorientable (i is odd).

Suppose, for more definiteness, that $p_1(\mu)$ lies above W^s_i. Evidently, for some μ^*, $P_1(\mu^*) \in W^s(M_i\bar{k})$. Then, $T_jS_j \cap W^s(M_{i\bar{k}}) \neq \emptyset$ at $\mu = \mu^*$ for any $j \geq i$. Since $\mathrm{lt}_{n\to\infty} T^n_{ik}S_j = W^s_i$, there exists an integer N such that the first return map on the set $T^{\bar{k}}_0 \circ T^N_{i\bar{k}} \cup^{\infty}_{j=i} S_j$ acts as a Smale horseshoe map on each pair of adjoining regions S_j and S_{j+1} (Figure 11).

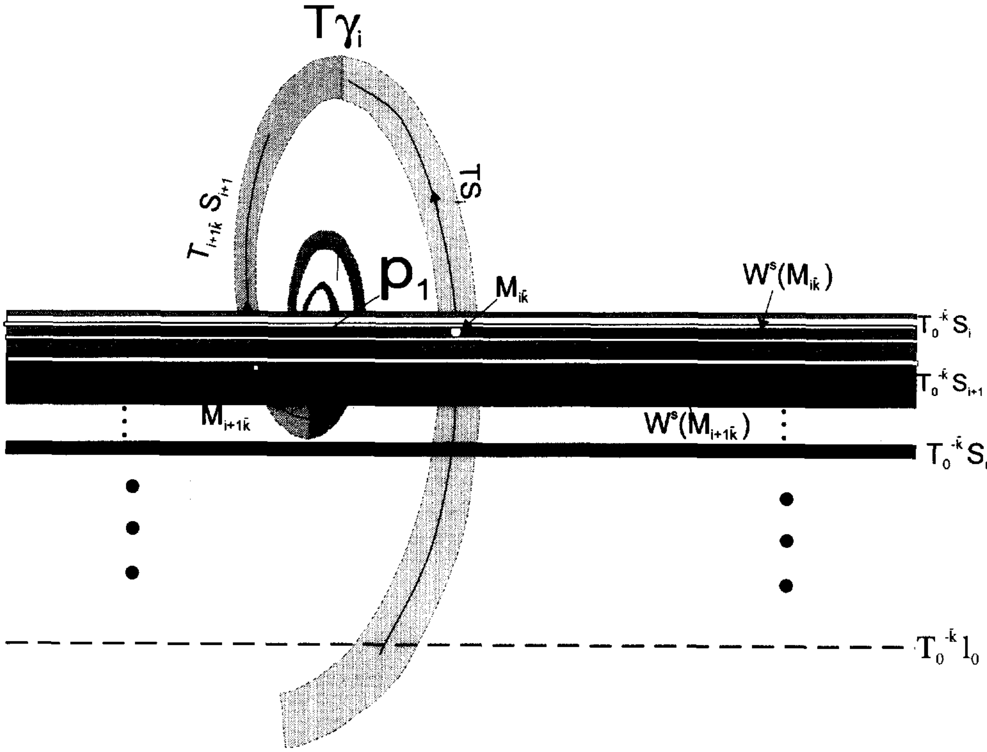

Figure 11. The existence of infinitely many Smale's horseshoes at the moment when the one-dimensional separatrix of the saddle-focus belongs to the stable manifold of the saddle periodic orbit lying in the region $T_0^{-\bar{k}}S_i$.

For μ close to μ^*, a large finite number m of the horseshoes is preserved. Therefore, for all close μ, in the set $T^{\bar{k}}_0 \circ T^n_{i\bar{k}}(S_j \cup S_{j+1})$, $i \leq j \leq i+m$, there exists a Cantor set $\mathcal{M}^n_{\mathrm{im}}(\mu)$ of stable invariant fibers of a nontrivial hyperbolic set which, in turn, serve as limits for sequences of the lines $\mathcal{L}^n_{\mathrm{im}}$ of preimages of the discontinuity line l_0. When μ varies, the point $p_1(\mu)$ intersects all these lines and each intersection corresponds to one of the bifurcation prescribed by the theorem. The theorem is proved.

5. THE DEATH OF THE SPIRAL QUASIATTRACTOR

After the bifurcation of the appearance of the heteroclinic orbit L_g that belongs to the intersection of the unstable manifold of a saddle periodic orbit and the stable manifold of the saddle-focus O, the set $T^+h_0 \in D^- \cap D_1$ (analogous to the set h^-_0 in D^-) will be mapped into $D^+ \cap D_2$ and its image by the map T^+ will have a spiral shape, winding to the point $p_1(\mu)$, and will lie in $D^+ \cap D_1$. When the distance to the bifurcational set in the parameter space that corresponds to the birth of the heteroclinic orbit L_g grows, the curves $T^+_0\gamma^+_0$ and $T^-_0\gamma^-_0$ will move far from the line l_0. Consequently, the set $h^+_0(h^-_0)$ will contain more and more preimages of the regions $S^-_j \cap D_1(S^+_j \cap D_2)$ corresponding to decreasing j. Finally, the moment happens when a structurally unstable heteroclinic orbit appears at the points of which the unstable manifold of the point M_{02} has a tangency with the stable manifold of the symmetric periodic orbit L (Figure 12). After that, the region D is no longer an absorbing domain because there appear regions in D for the points of which the stable periodic orbit Γ_0 is the limit set. These regions are the preimages of the region $G_0 \in h_0$ bounded by the curves $T_0^{-1}(S_0 \cap W^s(L_0)$ и $T_1^{-1}(S_1 \cap W^s(L_0)$.

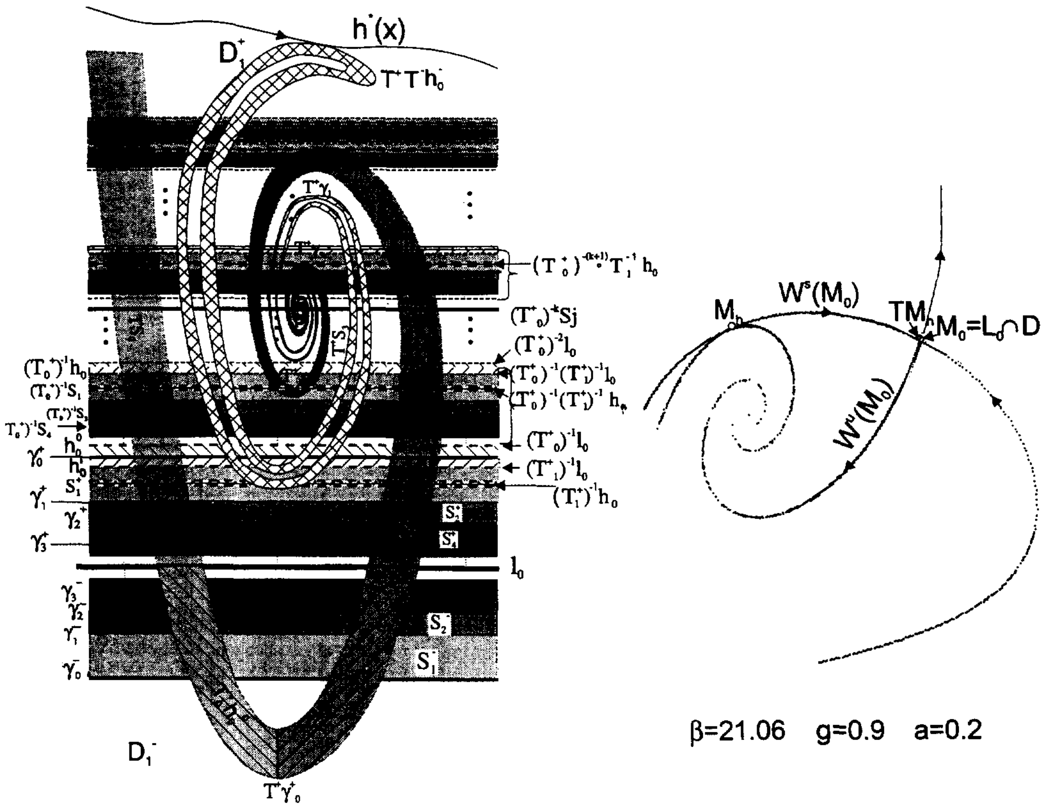

(a) The theoretical model.

(b) Computer simulations.

Figure 12. The moment of death of the double-scroll. Here, a heteroclinic orbit appears which tends to L_0 as $t \to \infty$, and tends, as $t \to -\infty$, to a saddle periodic orbit whose unstable manifold is the boundary of the nontrivial hyperbolic set. M_0 is the fixed point; $W^s(M_0)$ is the stable manifold of the fixed point M_0, $W^u(M_0)$ is the unstable manifold of the fixed point M_0; the points lying upper $W^s(M_0)$ tend to stable cycle Γ_0; M_h is the closed point to the nonrough heteroclinic point; TM_h is following iteration of the point M_h.

REFERENCES

1. V.S. Afraimovich, V.V. Bykov and L.P. Shil'nikov, On the appearance and structure of Lorenz attractor, *DAN SSSR* **234**, 336–339 (1977).
2. V.S. Afraimovich, V.V. Bykov and L.P. Shil'nikov, On the structurally unstable attracting limit sets of Lorenz attractor type, *Tran. Mosc. Soc.* **2**, 153–215 (1983).
3. V.S. Afraimovich and L.P. Shil'nikov, Strange attractors and quasi-attractors, In *Nonlinear Dynamics and Turbulence*, (Edited by G.I. Barenblatt, G. Iooss and D.D. Joseph), pp. 1–28, Pitman, New York, (1983).
4. V.S. Afraimovich and L.P. Shil'nikov, Invariant two-dimensional tori, their breakdown and stochastisity, In *Methods of Qualitative Theory of Differential Equations*, Gorky Univ. Press, (1983); translated in *Amer. Math. Soc. Trans.* **149** (2), 201–212 (1991).
5. L.P. Shil'nikov, The theory of bifurcations and turbulence 1, *Selecta Math. Sovietica* **1** (10), 43–53 (1991).
6. T. Matsumoto, L.O. Chua and M. Komuro, The double-scroll family, *IEEE Transaction on Circuits and Systems* **CAS-33** (11), 1073–1118 (1986).
7. T. Matsumoto, L.O. Chua and M. Komuro, Birth and death of the double-scroll, *Physica D* **24**, 97–124 (1987).
8. L.O. Chua and G. Lin, Intermittency in piecewise-linear circuit, *IEE Transaction and Systems* **38** (5) (1991).
9. D.P. George, Bifurcations in a piecewice linear system, *Physics Letters A* **118** (1), 17–21 (1986).

10. E. Freire, A.J. Rodriquez-Luis, E. Gamero and E. Ponce, A case study for homoclinic chaos in an autonomous electronic circuit, *Physica D* **62**, 230–253 (1993).
11. L.P. Shil'nikov, A contribution to the problem of a rough equilibrium state of saddle-focus type, *Math. USSR Sbornik* **10**, 92–103 (1970).
12. I.M. Ovsyannikov and L.P. Shil'nikov, On systems with a saddle-focus homoclinic curve, *Math. USSR Sbornik* **58**, 91–102 (1987).
13. N.K. Gavrilov and L.P. Shilnikov, On three-dimensional systems close to systems with a structurally unstable homoclinic curve 1, *Math. USSR Sb.* **17**, 446–485 (1973).
14. S.E. Newhouse, The abundance of wild hyperbolic sets and non-smooth stable sets for diffeormorphism, *Publ. Math., IHES* **50**, 101–151 (1979).
15. L.P. Shil'nikov, Chua's circuit: Rigorous results and future problems, *International Journal of Bifurcation and Chaos* **4** (3), 489–519 (1994).
16. E.I. Harozov, Versal unfolding of equivariant vector fields for the cases of the symmetry of the second and third orders, (in Russian), *Trans. of I.G. Petrovsky's Seminar* **5**, 163–192 (1979).
17. V.I. Arnold, *Geometrical Methods in the Theory of Ordinary Differential Equations*, Springer, New York, (1982).
18. L.A. Belyakov, Bifurcation of systems with homoclinic curve of saddle-focus, *Math. Notes of Academy of Sciences of USSR* **36** (1/2), 838–843 (1984).
19. A.S. Dmitriev, Yu.A. Komlev and D.V. Turaev, Bifurcation phenomena in the 1:1 resonant horn for the forced van der Pol-Duffing equations, *Bifurcation and Chaos* **2** (1) (1992).
20. R. Lozi and S. Ushiki, Confinor and bounded-time patterns in Chua's circuit and the double-scroll family, *International Journal of Bifurcation and Chaos* **1** (1), 119–138 (1991).
21. R. Lozi and S. Ushiki, The theory of confinors in Chua's curcuit: Accurate analisis of bifurcations and attractors, *International Journal of Bifurcation and Chaos* **3** (2), 333–361 (1993).
22. M.V. Shashkov and L.P. Shil'nikov, On existence of a smooth invariant foliation for maps of Lorenz type, (in Russian), *Differenzial'nye Uravnenija* **30** (4), 586–595 (1994).
23. V.I. Afraimovich and L.P. Shil'nikov, The singular sets of Morse-Smale systems, *Tran. Mosc. MATH, Soc.* **28**, 181–214 (1973).
24. J.A. Feroe, Homoclinic orbits in a parametrized saddle-focus system, *Physica D* **62** (1–4), 254–262 (1993).
25. T. Matsumoto, L.O. Chua and M. Komuro, The double-scroll, *IEE Trans.* **CAS-32**, 797–818 (1985).
26. L.P. Shil'nikov, On a Poincaré-Birkgoff problem, *Math. USSR Sborn.* **3**, 353–371 (1968).